

The contribution of protease-activated receptor 1 to neuronal damage caused by transient focal cerebral ischemia

Candice E. Junge^{*††}, Taku Sugawara[§], Guido Mannaioni^{*}, Sudar Alagarsamy[¶], P. Jeffrey Conn^{||}, Daniel J. Brat^{**}, Pak H. Chan[§], and Stephen F. Traynelis^{*‡}

Departments of ^{*}Pharmacology and ^{**}Pathology, Emory University, Atlanta, GA 30322; [§]Department of Neurosurgery, Stanford University, Palo Alto, CA 94305, [¶]Ferring Research Institute, Inc., San Diego, CA 92121; and ^{||}Department of Pharmacology, Vanderbilt University, Nashville, TN 37235

Communicated by Stephen F. Heinemann, The Salk Institute for Biological Studies, La Jolla, CA, August 29, 2003 (received for review March 4, 2003)

The serine proteases tissue plasminogen activator, plasmin, and thrombin and their receptors have previously been suggested to contribute to neuronal damage in certain pathological situations. Here we demonstrate that mice lacking protease-activated receptor 1 (PAR1) have a 3.1-fold reduction in infarct volume after transient focal cerebral ischemia. Intracerebroventricular injection of PAR1 antagonist BMS-200261 reduced infarct volume 2.7-fold. There are no detectable differences between PAR1^{-/-} and WT mice in cerebrovascular anatomy, capillary density, or capillary diameter, demonstrating that the neuroprotective phenotype is not likely related to congenital abnormalities in vascular development. We also show that the exogenously applied serine proteases thrombin, plasmin, and tissue plasminogen activator can activate PAR1 signaling in brain tissue. These data together suggest that if blood-derived serine proteases that enter brain tissue in ischemic situations can activate PAR1, this sequence of events may contribute to the harmful effects observed. Furthermore, PAR1 immunoreactivity is present in human brain, suggesting that inhibition of PAR1 may provide a novel potential therapeutic strategy for decreasing neuronal damage associated with ischemia and blood-brain barrier breakdown.

Protease-activated receptors (PARs) are G protein-coupled receptors that are activated by proteolytic cleavage of their N terminus, which unmask an amino acid sequence that acts as a tethered ligand to activate the receptor (1, 2). PAR1 mRNA is distributed widely throughout young and adult brain tissue (3–5), and it has recently been demonstrated that PAR1 protein is present in the adult rat brain and up-regulated after experimental ischemia in hippocampal slice cultures (5, ††). PAR1 activation has been suggested to mediate several pathological effects, including neurite retraction (6–8), cell death in hippocampal cultures and motoneurons (7, 9, 10), and potentiation of *N*-methyl-D-aspartate (NMDA) receptor responses (11).

Plasma-derived serine proteases that function in the clotting/fibrinolysis cascade such as tissue plasminogen activator (tPA), plasmin, and thrombin do not normally enter brain tissue because of the blood-brain barrier (BBB). Several animal models of cerebral insult show that large proteins such as tPA and albumin (12) do enter brain tissue during BBB breakdown (13). Furthermore, both tPA and plasminogen proteins are expressed in the mouse hippocampus (14). Plasmin and thrombin both can activate PAR1 (11, 15, 16). Plasmin, which is generated from tPA's cleavage of plasminogen, has been implicated together with tPA in neuronal death in certain pathological situations. The substrate through which the tPA/plasmin system exerts its harmful effects, however, remains unknown. In an animal model of transient focal ischemia, tPA^{-/-} mice exhibited an 8-fold reduction in cell death in the hippocampal CA1–CA3 subfields compared with WT mice. tPA administration to both WT and tPA^{-/-} mice dramatically increased the size of cerebral infarction (13, ‡‡). These findings have interesting implications

for situations in which disruption of the BBB allows higher concentrations of blood-derived serine proteases and zymogen precursors to enter the brain, which may cause aberrant activation of serine protease signaling with deleterious consequences (12). Potentially harmful effects of tPA are relevant for stroke patients who are administered tPA intravenously as a thrombolytic agent to facilitate reperfusion of ischemic tissue. Because PAR1 could be activated by blood-derived plasmin and thrombin, we used a murine stroke model of transient focal ischemia to determine whether PAR1 signaling contributes to cell death.

Methods

Phosphoinositide (PI) Hydrolysis. PI hydrolysis was measured as described (17, 18).

Transient Focal Cerebral Ischemia. Transient focal cerebral ischemia was induced by intraluminal middle cerebral artery (MCA) blockade with a monofilament suture. All procedures involving animals were approved by Emory University Institutional Animal Care and Use Committee. Male C57BL/6 mice (3–5 months, The Jackson Laboratory), or PAR1^{-/-} (19) and littermate WT mice (>99% C57BL/6) were anesthetized with 2% isoflurane in 30% O₂ and 70% NO. The rectal temperature was controlled at 37°C with a homeothermic blanket. The femoral artery was cannulated to monitor blood pressure and measure arterial blood gases (Chiron). Relative changes in regional cerebral blood flow were monitored with a laser Doppler flowmeter (Vasamedic, Minneapolis). An 11-mm 5-0 dermalon nylon suture was introduced into the left internal carotid artery through the external carotid artery stump. After 30-min MCA occlusion, blood flow was restored by withdrawing the suture. After 24-h survival, the brain was removed and cut into 2-mm sections. The lesion was identified with 2% 2,3,5-triphenyltetrazolium chloride (TTC) in PBS at 37°C for 20 min. The infarct area of each section was measured two different ways by using NIH IMAGE (Scion Corporation, Beta 4.0.2 release) and multiplied by the section thickness to give the infarct volume.

Abbreviations: BBB, blood-brain barrier; tPA, tissue plasminogen activator; NMDA, *N*-methyl-D-aspartate; PAR, protease-activated receptor; MCA, middle cerebral artery; TTC, 2,3,5-triphenyltetrazolium chloride; PI, phosphoinositide.

†To whom correspondence should be addressed. E-mail: cjunge@ucla.edu.

‡A patent is pending on "Treatment of neurodegenerative diseases and conditions using PAR1 antagonists," and S.F.T. and C.E.J. are coinventors on that patent.

††Neurons and glia express zymogen precursors to serine proteases (32–34), as well as several unique serine proteases, including neurotrypsin (35) and neuropsin (36).

‡‡tPA^{-/-} mice similarly suffer minimal cell death in the hippocampus after intrahippocampal injection of kainic acid (a glutamate receptor agonist), whereas WT mice experienced nearly complete cell loss (37, 38). Furthermore, plasminogen^{-/-} mice that underwent the same experimental procedure were also resistant to neuronal loss in the hippocampus when compared with WT mice (39). These data suggest that tPA activation of plasminogen to plasmin is required for neuronal death after excitotoxic injury induced by kainic acid.

© 2003 by The National Academy of Sciences of the USA

Table 1. PI hydrolysis (fold over basal) in mouse hippocampal slices

	WT	PAR ^{-/-}	Plasminogen ^{-/-}
Thrombin (30 nM)	1.80 ± 0.15*	0.95 ± 0.20	1.7 ± 0.14*
Plasmin (200 nM)	2.01 ± 0.2*	0.85 ± 0.2	–
tPA (30 μg/ml)	1.51 ± 0.13*	1.14 ± 0.12	1.0 ± 0.15
tPA (30 μg/ml) + α2-antiplasmin (1 μM)	1.2 ± 0.14	–	–

All measurements were performed in at least three animals and represent triplicate measures in each animal (mean ± SEM). Unpaired *t* tests were performed to determine significance.

*Significant increase in PI hydrolysis compared with basal PI hydrolysis levels (*P* < 0.05).

First, the density slice option in NIH IMAGE was used to segment the images based on standard intensity selected from the most severely damaged area in a WT lesion. This standard was maintained throughout the analysis, and only objects at this intensity were highlighted for area measurement. Second, the area of the lesion, as identified by reduced TTC staining, was manually circled. A ratio of the contralateral to ipsilateral hemisphere section volume was multiplied by the corresponding infarct section volume to correct for edema.

Intracerebroventricular Injection. The PAR1 antagonist BMS-200261 in Hepes-buffered saline (HBS, 10 mM Hepes, 0.9% NaCl), peptide 68 in HBS/DMSO (50% vol), or appropriate vehicle was injected into the right ventricle (2 mm posterior and 1 mm lateral of the bregma, needle inserted 3 mm) of male C57BL/6 mice (3–5 months old, The Jackson Laboratory) 30 min before MCA occlusion surgery. BMS-200261 and peptide 68 were synthesized (Emory University Microchemical Facility) with a trifluoroacetic acid counterion and were diluted in HBS to ensure neutral pH. Mice were anesthetized with 3.0% isoflurane in 30% O₂ and 70% NO (in some cases nitrous oxide was not used) and placed in a stereotaxic apparatus. One microliter of BMS-200261, peptide 68, or appropriate vehicle was injected into the ventricle. Mice were killed 24 h after MCA occlusion surgery and the lesion was identified and analyzed as described above. Mice with subarachnoid hemorrhages were excluded.

BBB Breakdown. Evans blue (2%, Sigma) in saline was injected into the left jugular vein immediately before MCA occlusion surgery. Mice were killed 4 h after surgery and transcardially perfused with 4% paraformaldehyde. Brains were sectioned into 50-μm sections by using a vibratome (Leica), and Evans blue leakage into brain tissue was visualized under a fluorescent microscope (excitation = 355 nm; emission >415 nm). Optical density measurements in the striatum were performed by using NIH IMAGE. Nuclei were counterstained with 4',6-diamidino-2-phenylindole (Sigma).

Electron Microscopy. Mice were anesthetized with 1.0 g/kg chloral hydrate and perfused transcardially with 3% paraformaldehyde and 0.2% glutaraldehyde in 0.1 M phosphate buffer (PB). Brains were removed 1 h after perfusion and sectioned at 50 μm by using a vibratome. Polyclonal primary antibodies against glial fibrillary acidic protein (GFAP, Dako) were used at 1:2,000 to 1:4,000 dilutions, and biotinylated goat anti-rabbit secondary antibodies at 1:200 (Vector Laboratories). To visualize GFAP immunoreactivity, the avidin-biotin complex (ABC Elite, Vector Laboratories) method was used. Brain sections were prepared for electron microscopic analysis as described (20, 21). Capillary lumen area was measured by using NIH IMAGE.

Immunohistochemistry in Mouse Brain Tissue. Brains were fixed in 10% buffered formalin, routinely processed, paraffin embedded, and sectioned at 6 μm. Sections were deparaffinized and exposed to heat induced epitope retrieval by steaming for 15 min. Sections were incubated at room temperature with Factor VIII antibody (prediluted, rabbit polyclonal, DAKO) or GFAP (1:100, mouse monoclonal, DAKO) and appropriate blocking reagents (animal research kit, DAKO). The avidin biotin complex method (ABC Elite) was used to visualize immunoreactivity.

Immunohistochemistry in Human Tissue. Postmortem human brain was retrieved from the autopsy service of Emory University hospital within 4 h of death. Frontal lobe, striatum, and temporal lobe including hippocampus were fixed in 3% paraformaldehyde for 48 h and then cryoprotected in 30% sucrose in 0.1 M phosphate buffer. Brain tissue was frozen on dry ice and cut at 40 μm on a sliding microtome. A PAR1 monoclonal antibody (2.5 μg/ml, WEDE15, Beckman Coulter) and a biotin-conjugated rat anti-mouse secondary antibody (1:200, Jackson ImmunoResearch) were used with the avidin-biotin complex method. To verify antibody specificity, primary or secondary antibody was omitted and no immunostaining was observed. The primary antibody was preadsorbed with the control peptide and no immunostaining was observed.

Table 2. Average physiological parameters measured before, during, and after MCA occlusion surgery in subset of animals

	pH	pCO ₂ , mmHg	pO ₂ , mmHg	BP (mean), mmHg	Temperature, °C	% Decrease in CBF
WT (<i>n</i> = 4)						
Before occlusion	7.4 ± 0.02	29.4 ± 3.0	179.0 ± 15.9	78.3 ± 4.3	37.2 ± 0.2	
During occlusion	7.38 ± 0.02	33.3 ± 1.7	165.3 ± 13.3	79.3 ± 5.4	37.0 ± 0.1	80.1 ± 3.4
After occlusion	7.34 ± 0.02	38.6 ± 3.2	151.0 ± 11.7	73.8 ± 4.3	36.9 ± 0.1	
PAR1 ^{-/-} (<i>n</i> = 4)						
Before occlusion	7.38 ± 0.01	32.0 ± 2.2	166.6 ± 15.8	84.5 ± 6.3	36.9 ± 0.1	
During occlusion	7.35 ± 0.04	33.3 ± 4.9	159.8 ± 23.1	85.0 ± 8.3	36.9 ± 0.2	78.4 ± 2.3
After occlusion	7.33 ± 0.04	34.3 ± 2.6	163.7 ± 15.8	69.0 ± 9.7	37.1 ± 0.2	

Cerebral blood flow (CBF) measurements were recorded 5 min after MCA occlusion. There were no statistically significant differences (ANOVA) in any of the parameters between PAR1^{-/-} and WT mice. 1 mmHg = 133 Pa.

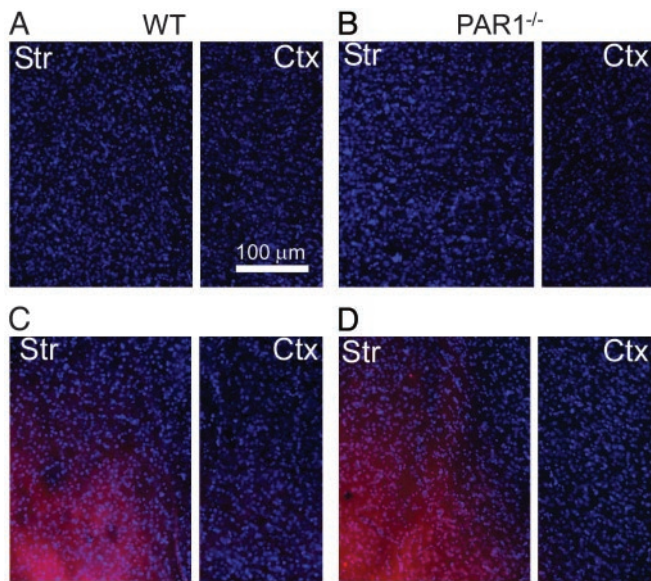


Fig. 3. Evans blue images of coronal sections from WT and $PAR1^{-/-}$ mice. (A and B) Fluorescent images (excitation = 355 nm and emission >415 nm) of 50- μ m sections after sham surgery (nonischemic conditions) from WT ($n = 2$) and $PAR1^{-/-}$ ($n = 2$) mice showing no Evans blue entry into striatum (str) and cortex (ctx). (C and D) Fluorescent images of 50- μ m sections from WT ($n = 4$) and $PAR1^{-/-}$ ($n = 4$) striatum and cortex after 30 min of MCA occlusion showing similar Evans blue entry into brain tissue.

activation contributes to cell death after ischemia, we performed transient MCA occlusion surgeries in $PAR1^{-/-}$ and WT mice. The left MCA was occluded for 30 min, which reduced blood flow to the left hemisphere by $\approx 80\%$ (Table 2). Reperfusion was allowed for 24 h. The mice were then killed, and the lesion area was identified by using the vital dye TTC (Fig. 1A and C). To directly compare the level of damage after MCA occlusion between the WT and $PAR1^{-/-}$ mice, the grayscale scanned brain section images were segmented on the basis of intensity (Fig. 1A). When the most damaged area of the WT lesion was used as the standard, the lesion volume was calculated without subjective bias for WT and $PAR1^{-/-}$ mice. This analysis showed that $PAR1^{-/-}$ mice had a 3.1-fold reduction in infarct volume (Fig. 1B, 27.1 ± 6.1 mm³, $P < 0.005$ Mann–Whitney test) compared with the WT mice (83.8 ± 11.1 mm³). We also took a more conservative approach to determine the infarct volume by measuring the core of the infarct as well as more penumbral regions in which the neuronal degeneration was only slight, as judged by reduced intensity of TTC stain. $PAR1^{-/-}$ mice again showed a significant reduction in total infarct volume (Fig. 1D, 47.5 ± 8.2 mm³, $P < 0.005$, Mann–Whitney test) compared with WT mice (97.3 ± 9.7 mm³). No differences were observed in physiological parameters monitored before, during, and after the surgery in a subset of WT and $PAR1^{-/-}$ mice (Table 2).

Because there are multiple processes that contribute to neurodegeneration during prolonged periods of ischemia that may overshadow neuroprotective manipulations (24, 25), we chose a brief 30-min duration of MCA occlusion to produce a submaximal degree of ischemic damage. Consistent with this idea, we did not observe a neuroprotective effect in $PAR1^{-/-}$ mice after 1 h of ischemia (data not shown, $n = 5$), which further supports the concept that there are multiple parallel processes of cell death during prolonged ischemia.

Analysis of WT and $PAR1^{-/-}$ Brain Anatomy and Vasculature. To ensure there were no obvious differences in the cerebrovascu-

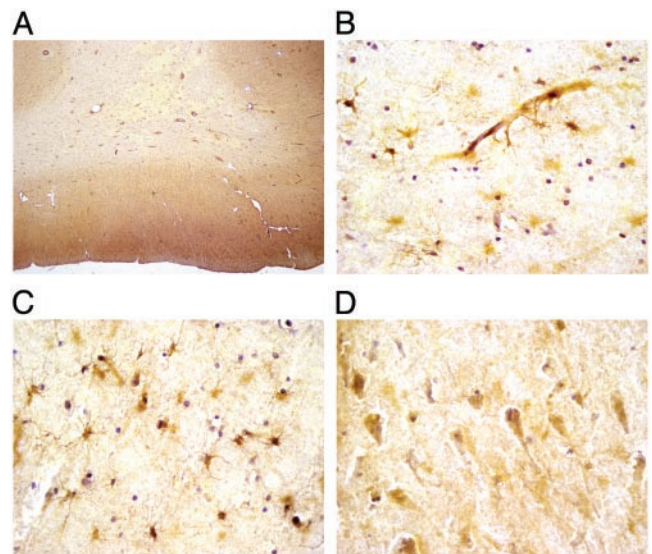


Fig. 4. $PAR1$ immunostaining (hematoxylin counterstained) in human brain tissue ($n = 3$). (A) Low-magnification image of human frontal lobe. The cerebral cortex shows mild immunostaining of both neuropil and neuronal cell bodies compared with the white matter, which shows very little immunoreactivity except for individual astrocytes. (B) Immunostained capillary and astrocytes in temporal lobe. (C) Immunostained astrocytes in white matter show immunoreactivity in the cell body and processes. Oligodendrocytes and axonal processes do not show immunostaining. (D) Large pyramidal neurons in temporal lobe are preferentially stained compared with medium to smaller sized neurons.

lature that might account for the differential sensitivity to experimental ischemia, WT and $PAR1^{-/-}$ mice were perfused with 2% carbon black in 20% gelatin in water to evaluate the major vessels. We observed no obvious differences in vascular anatomy between WT and $PAR1^{-/-}$ mice with regard to the circle of Willis and its major branches (data not shown, $n = 4$).

To compare cellular morphology, brain anatomy, and vascular density, WT and $PAR1^{-/-}$ standard histological brain sections were analyzed both qualitatively and quantitatively. Because most of the damage after MCA occlusion occurs in the striatum, hippocampus and cortex, our analysis focused on these brain regions. Histological sections revealed no apparent vascular malformations or structural abnormalities in $PAR1^{-/-}$ brains ($n = 5$, data not shown). Factor VIII immunostaining and histological examination revealed that endothelial cells, capillaries, perivascular cells and spaces appeared normal (Fig. 2A and B). Furthermore, there were no observable differences in GFAP staining of adjacent astrocytes at the light and electron microscopic levels, suggesting that both WT and $PAR1^{-/-}$ capillaries are similarly invested by astrocytic endfeet (Fig. 2C and D).

Although the standard histological sections revealed no evident differences between WT and $PAR1^{-/-}$ mice at the cellular and anatomical levels, ultrastructural analysis of brain capillaries was performed to evaluate some elements of the BBB.⁵⁸ Capillaries from the CA1 region of the hippocampus, the striatum and the cortex from five WT ($n = 100$ capillaries) and five $PAR1^{-/-}$ ($n = 100$ capillaries) mice were analyzed for the presence of tight junctions, endothelial cell morphology, and

⁵⁸The analysis of cerebrovasculature is important because BBB breakdown is a principal step in the pathological process during and after ischemia. It is well documented in animal models of ischemia that the permeability of the BBB increases, allowing extravasation of small molecules and blood proteins into brain tissue and resulting in damage to neuronal cells (12, 40–43).

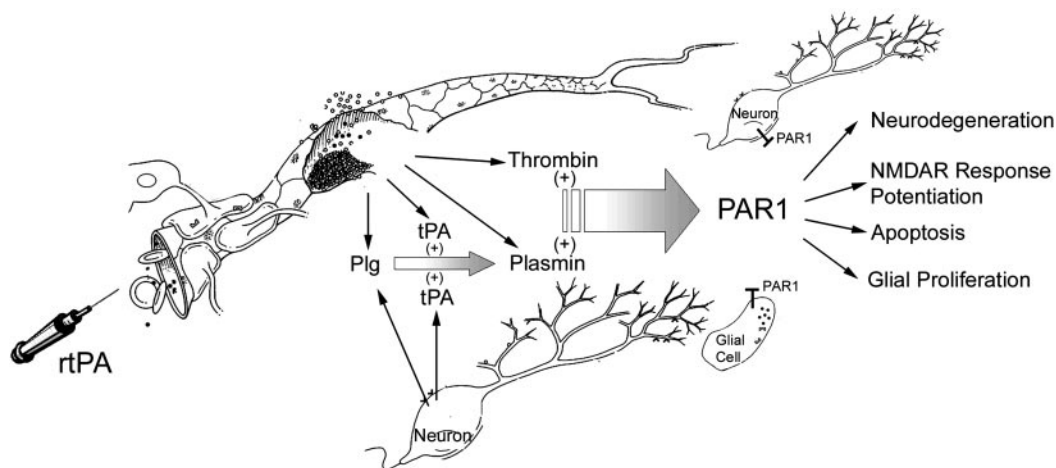


Fig. 5. Mechanism and consequences of PAR1 activation during BBB breakdown. Both thrombin and plasmin can enter brain tissue and activate PAR1 with deleterious consequences. Plasminogen (Plg) and tPA (either endogenous or therapeutically administered, rtPA) can (i) enter brain from the blood or (ii) be released from neurons. Once in the brain, plasminogen and tPA, regardless of the source, can produce plasmin, which can activate PAR1.

astrocytic endfeet contact with endothelial cells. Both WT and PAR1^{-/-} mice had one to two endothelial cells forming the capillary with a basal lamina of similar thickness surrounding them (Fig. 2E and F). The tight junctions appeared similar and were observed in WT and PAR1^{-/-} mice. WT and PAR1^{-/-} capillaries showed GFAP staining around the capillary, suggesting astrocytic endfeet similarly contact the basal lamina. We could find no qualitative differences between WT and PAR1^{-/-} capillaries.

Quantification of Vascular Characteristics. There were no differences between the WT and PAR1^{-/-} vascular densities in the striatum, hippocampus, and cortex ($P > 0.05$, ANOVA) suggesting there was no additional blood supply to these regions in the PAR1^{-/-} mice that could account for the reduction in infarct volume (Fig. 2G). Capillaries were identified by the presence of Factor VIII immunostaining of endothelial cells within vascular profiles. Furthermore, there were no differences ($P > 0.05$, unpaired *t* test) observed in capillary lumen area between WT and PAR1^{-/-} mice (Fig. 2G). These results together suggest that the PAR1^{-/-} mice did not experience increased neuroprotection due to increased blood volume in or blood flow to the striatum, hippocampus, or cortex.

PAR1 Antagonist Reduces Infarct Volume. To further verify that the neuroprotection observed in PAR1^{-/-} mice was not caused by a developmental abnormality, we tested whether inhibition of PAR1 decreased damage after MCA occlusion by using the PAR1 antagonist BMS-200261 and a structurally related 1000-fold less potent analogue, peptide 68 (26). BMS-200261 (1 μ M) blocked PAR1-mediated PI hydrolysis ($n = 3$, data not shown) stimulated by the agonist peptide TFLLR-NH₂ (Thr-Phe-Leu-Leu-Arg) treatment of hippocampal slices. We injected 1 μ l of either HBS or BMS-200261 (2 or 6 mM, dilution of 1:200 throughout the brain would place the interstitial concentration in the range of 10 or 30 μ M) in HBS into the lateral ventricle 30 min before MCA occlusion. Injection of 6 mM BMS-200261 ($n = 6$) significantly reduced infarct volume (23.4 ± 9.5 mm³, $P < 0.05$ nonparametric ANOVA) compared with HBS-injected mice (63.1 ± 8.0 mm³, $n = 15$, Fig. 2H). To verify that the neuroprotection observed was caused by selective inhibition of PAR1, experiments were repeated with peptide 68 or vehicle. No significant differences in infarct volume were observed between mice injected with vehicle (69.4 mm³ \pm 23, $n = 6$, data not shown) or peptide 68 (80.9 mm³ \pm 11, $n = 6$, $P > 0.05$ Mann-Whitney test).

Evaluation of BBB Breakdown. Although we could not detect any differences between the BBB of WT and PAR1^{-/-} mice, it is possible that, during ischemia, the BBB in PAR1^{-/-} mice did not breakdown to the same extent as in WT mice because of factors undetectable at the ultrastructural level. Because PAR1 is expressed on endothelial as well as smooth muscle cells (1), we evaluated Evans blue entry into WT or PAR1^{-/-} brain tissue in ischemic and nonischemic conditions to test whether PAR1 played a role in BBB breakdown (Fig. 3). Mice that underwent a sham surgery or MCA occlusion for 30 min were killed 4 h after surgery to quantify Evans blue entry into the brain tissue.¹¹ Optical density (OD) measurements of Evans blue fluorescence revealed an equal amount of Evans blue entry into the ipsilateral hemisphere (Fig. 3C and D) of WT ($n = 4$) and PAR1^{-/-} ($n = 4$) mice, which suggests there were no detectable differences in BBB breakdown (WT = 193.7 ± 9.0 OD, PAR1^{-/-} = 188.1 ± 7.6 OD, $P > 0.05$ unpaired *t* test, mean \pm SEM). No Evans blue fluorescence was observed in the contralateral hemisphere (data not shown) or in the nonischemic animals (Fig. 3A and B, WT $n = 2$, PAR1^{-/-} $n = 2$), indicating that the BBB was intact for both groups.

PAR1 Protein Localization in Human Brain. Our finding that PAR1 appears to be an early contributor to neurodegeneration after experimental ischemia suggests that PAR1 may be a potential therapeutic target for stroke or brain injury patients. Although PAR1 protein is expressed in mouse and rat CNS (see above), PAR1's protein distribution in human brain is unknown. Therefore, we investigated the PAR1 protein distribution in human brain regions that are sensitive to ischemia and commonly injured after stroke. Western blots of human cortex and hippocampus ($n = 5$) that were probed with a monoclonal antibody (WEDE15) made to human PAR1 revealed a 66-kDa band (Fig. 6, which is published as supporting information on the PNAS web site, www.pnas.org) which corresponds to previous reports of PAR1's molecular weight (27, 28). In general, gray matter showed higher PAR1 immunoreactivity than white matter. Within the cortex ($n = 3$), striatum ($n =$

¹¹Evans blue (2%) in saline was injected into the jugular vein of WT ($n = 4$) and PAR1^{-/-} ($n = 4$) mice immediately before the MCA occlusion surgery. Evans blue is a 2-kDa molecule that is normally restricted to the vascular space in the CNS but can cross the BBB during experimental ischemia (12). The 4-h time point was chosen because previous studies have established that BBB breakdown does occur at this point after MCA occlusion (44). At later time points, multiple factors likely contribute to BBB breakdown, making interpretation of the data more complex.

3, data not shown), and hippocampus ($n = 3$, data not shown), larger neurons and astrocytes are preferentially stained (Fig. 4). The neuropil, which consists of the delicate meshwork of glial and neuronal processes, shows mild staining. Within white matter, only astrocytes exhibit intense staining (Fig. 4 B and C). Neither white matter oligodendrocytes nor axonal processes show any appreciable immunoreactivity. Ependymal cells lining the lateral ventricles also do not show staining (data not shown). Blood vessels and capillaries in the brain tissue exhibit PAR1 immunostaining (Fig. 4 A and B), consistent with previous reports that PAR1 is present on endothelial cells (29). The expression of PAR1 in human brain suggests that the neuroprotective effects of inhibiting PAR1 activation observed in mice may be relevant for humans.

Discussion

The most important findings of this study are that both the lack of PAR1 and pharmacological blockade of PAR1 confer significant neuroprotection after transient focal cerebral ischemia. These data suggest that PAR1 activation has an important role in mediating neurodegeneration in ischemic situations. Although blood-derived thrombin is one potential activator of PAR1, other proteases such as plasmin may also activate PAR1 during ischemia. In recent years, the tPA/plasmin system has been under increased scrutiny because tPA is used as thrombolytic therapy for a subset of stroke patients, which may result in elevated concentrations of tPA and plasmin in brain tissue. Our data indicate that these serine proteases can initiate PAR1 signaling in brain tissue, which may contribute to the pathological processes in situations in which the BBB is compromised (Fig. 5).

PAR1 has recently been shown to be involved in blood vessel formation (30) and is expressed on smooth muscle and endothelial

cells. Our data indicate that the neuroprotective effects observed in PAR1^{-/-} mice do not result from developmental vascular abnormalities that would increase blood flow to brain regions most sensitive to ischemia. In addition, PAR1 is not expressed on mouse platelets; therefore, inhibition of clotting does not mediate the neuroprotection observed. Because we did not find any differences between the WT and PAR1^{-/-} mice in ischemic BBB breakdown, PAR1 is most likely initiating signaling cascades at the neuronal or glial level that compromise cell survival. PAR1 activation has been shown to potentiate NMDA receptor responses and cause apoptosis in neurons, both of which contribute to the pathological process after experimental ischemia (22–24, 31). Thus, there are multiple ways that PAR1 could exacerbate ischemic damage. Our finding that PAR1 is expressed in human neurons and glia suggests that PAR1's role in this rodent model of ischemia may be relevant for ischemia in humans. Therefore, inhibiting PAR1 activation may provide a new therapeutic strategy for stroke and situations in which the BBB is compromised.

We thank Sean Coughlin for generously sharing PAR1^{-/-} mice, Polina Lyuboslavsky for technical assistance, Hong Yi and the Emory University Electron Microscopy Core Facility for their help with the ultrastructural analysis, the Emory University Microchemical Facility for synthesis of BMS-200261 and related peptides, and Takeshi Hyashi for assistance with the intracerebroventricular injections. S.F.T. was supported by National Institutes of Health (NIH) Grant NS 39419 and the National Alliance for Research on Schizophrenia and Depression (NARSAD); C.E.J. was supported by NIH Grant NS 42505; P.J.C. was supported by NIH Grant MH 62646; G.M. was supported by NARSAD; D.J.B. was supported by NIH Grant NS 42934; and P.H.C. was supported by NIH Grants NS 14543, NS 25372, NS 36147, and NS 38653 and an American Heart Association Bugher Foundation Award.

- Macfarlane, S. R., Seatter, M. J., Kanke, T., Hunter, G. D. & Plevin, R. (2001) *Pharmacol. Rev.* **53**, 245–282.
- Hollenberg, M. D. & Compton, S. J. (2002) *Pharmacol. Rev.* **54**, 203–217.
- Niclou, S., Suidan, H. S., Brown-Luedi, M. & Monard, D. (1994) *Cell. Mol. Biol.* **40**, 421–428.
- Weinstein, J. R., Gold, S. J., Cunningham, D. D. & Gall, C. M. (1995) *J. Neurosci.* **15**, 2906–2919.
- Striggow, F., Riek-Burchardt, M., Kiesel, A., Schmidt, W., Henrich-Noack, P., Breder, J., Krug, M., Reymann, K. G. & Reiser, G. (2001) *Eur. J. Neurosci.* **14**, 595–608.
- Suidan, H. S., Stone, S. R., Hemmings, B. A. & Monard, D. (1992) *Neuron* **8**, 363–375.
- Turgeon, V. L., Lloyd, E. D., Wang, S., Festoff, B. W. & Houenou, L. J. (1998) *J. Neurosci.* **18**, 6882–6891.
- Gurwitz, D. & Cunningham, D. D. (1988) *Proc. Natl. Acad. Sci. USA* **85**, 3440–3444.
- Donovan, F. M., Pike, C. J., Cotman, C. W. & Cunningham, D. D. (1997) *J. Neurosci.* **17**, 5316–5326.
- Turgeon, V. L., Milligan, C. E. & Houenou, L. J. (1999) *J. Neuropathol. Exp. Neurol.* **58**, 499–504.
- Gingrich, M. B., Junge, C. E., Lyuboslavsky, P. & Traynelis, S. F. (2000) *J. Neurosci.* **20**, 4582–4595.
- Gingrich, M. B. & Traynelis, S. F. (2000) *Trends Neurosci.* **23**, 399–407.
- Wang, Y. F., Tsirka, S. E., Strickland, S., Stieg, P. E., Soriano, S. G. & Lipton, S. A. (1998) *Nat. Med.* **4**, 228–231.
- Tsirka, S. E., Rogove, A. D., Bugge, T. H., Degen, J. L. & Strickland, S. (1997) *J. Neurosci.* **17**, 543–552.
- Ishihara, H., Connolly, A. J., Zeng, D., Kahn, M. L., Zheng, Y. W., Timmons, C., Tram, T. & Coughlin, S. R. (1997) *Nature* **386**, 502–506.
- Kuliopulos, A., Covic, L., Seeley, S. K., Sheridan, P. J., Helin, J. & Costello, C. E. (1999) *Biochemistry* **38**, 4572–4585.
- Chung, D. S., Traynelis, S. F., Murphy, T. J. & Conn, P. J. (1997) *J. Pharmacol. Exp. Ther.* **283**, 742–749.
- Winder, D. G. & Conn, P. J. (1995) *J. Neurochem.* **64**, 592–599.
- Connolly, A. J., Ishihara, H., Kahn, M. L., Farese, R. V. J. & Coughlin, S. R. (1996) *Nature* **381**, 516–519.
- Hersch, S. M., Yi, H., Heilman, C. J., Edwards, R. H. & Levey, A. I. (1997) *J. Comp. Neurol.* **388**, 211–227.
- Hersch, S. M., Ciliax, B. J., Gutekunst, C. A., Rees, H. D., Heilman, C. J., Yung, K. K., Bolam, J. P., Ince, E., Yi, H. & Levey, A. I. (1995) *J. Neurosci.* **15**, 5222–5237.
- Choi, D. (1998) *Mt. Sinai J. Med.* **65**, 133–138.
- Lees, K. R. (1997) *Neurology* **49**, S66–S69.
- Muir, K. W. & Lees, K. R. (1995) *Stroke* **26**, 503–513.
- De Keyser, J., Sulter, G. & Luiten, P. G. (1999) *Trends Neurosci.* **22**, 535–540.
- Bernatowicz, M. S., Klimas, C. E., Hartl, K. S., Peluso, M., Allegretto, N. J. & Seiler, S. M. (1996) *J. Med. Chem.* **39**, 4879–4887.
- Molino, M., Blanchard, N., Belmonte, E., Tarver, A. P., Abrams, C., Hoxie, J. A., Cerletti, C. & Brass, L. F. (1995) *J. Biol. Chem.* **270**, 11168–11175.
- Woolkalis, M. J., DeMelfi, T. M. J., Blanchard, N., Hoxie, J. A. & Brass, L. F. (1995) *J. Biol. Chem.* **270**, 9868–9875.
- Hamilton, J. R., Moffatt, J. D., Tatoulis, J. & Cocks, T. M. (2002) *Br. J. Pharmacol.* **136**, 492–501.
- Griffin, C. T., Srinivasan, Y., Zheng, Y. W., Huang, W. & Coughlin, S. R. (2001) *Science* **293**, 1666–1670.
- Graham, S. H. & Chen, J. (2001) *J. Cereb. Blood Flow Metab.* **21**, 99–109.
- Luthi, A., Van der Putten, H., Botteri, F. M., Mansuy, I. M., Meins, M., Frey, U., Sansig, G., Portet, C., Schmutz, M., Schroder, M., et al. (1997) *J. Neurosci.* **17**, 4688–4699.
- Nakajima, K., Tsuzaki, N., Nagata, K., Takemoto, N. & Kohsaka, S. (1992) *FEBS Lett.* **308**, 179–182.
- Sumi, Y., Dent, M. A., Owen, D. E., Seeley, P. J. & Morris, R. J. (1992) *Development (Cambridge, U.K.)* **116**, 625–637.
- Gschwend, T. P., Krueger, S. R., Kozlov, S. V., Wolfer, D. P. & Sonderegger, P. (1997) *Mol. Cell Neurosci.* **9**, 207–219.
- Chen, Z. L., Yoshida, S., Kato, K., Momota, Y., Suzuki, J., Tanaka, T., Ito, J., Nishino, H., Aimoto, S. & Kiyama, H. (1995) *J. Neurosci.* **15**, 5088–5097.
- Tsirka, S. E., Rogove, A. D. & Strickland, S. (1996) *Nature* **384**, 123–124.
- Tsirka, S. E., Gualandris, A., Amaral, D. G. & Strickland, S. (1995) *Nature* **377**, 340–344.
- Tsirka, S. E., Bugge, T. H., Degen, J. L. & Strickland, S. (1997) *Proc. Natl. Acad. Sci. USA* **94**, 9779–9781.
- Petty, M. A. & Wettstein, J. G. (2001) *Brain Res. Brain Res. Rev.* **36**, 23–34.
- Selmaj, K. (1996) *Springer Semin. Immunopathol.* **18**, 57–73.
- Rubin, L. L. & Staddon, J. M. (1999) *Annu. Rev. Neurosci.* **22**, 11–28.
- Kastrup, A., Engelhorn, T., Beaulieu, C., de Crespigny, A. & Moseley, M. E. (1999) *J. Neurol. Sci.* **166**, 91–99.
- Fujimura, M., Gasche, Y., Morita-Fujimura, Y., Massengale, J., Kawase, M. & Chan, P. H. (1999) *Brain Res.* **842**, 92–100.